Available online at www.sciencedirect.com

SCIENCE DIRECT®

Polymer 47 (2006) 1480–1485

polymer

www.elsevier.com/locate/polymer

An effective layer-by-layer adsorption and polymerization method to the fabrication of polyoxometalate-polypyrrole nanoparticle ultrathin films

Yang Lan [a], Enbo Wang [a,*], Yonghai Song [b], Yanli Song [a], Zhenhui Kang [a], Lin Xu [a], Zhuang Li [b]

[a] *Department of Chemistry, Institute of Polyoxometalate Chemistry, Northeast Normal University, Changchun, Jilin 130024, People's Republic of China*
[b] *State Key Laboratory of Electroanalytical Chemistry, Changchun Institute of Applied Chemistry, Chinese Academy of Sciences, Jilin 130022, People's Republic of China*

Received 26 July 2005; received in revised form 23 November 2005; accepted 1 December 2005
Available online 10 January 2006

Abstract

A layer-by-layer (LbL) adsorption and polymerization method was developed for the controllable preparation of polypyrrole (PPy) nanoparticles within ultrathin films. By repetitive adsorption of pyrrole and subsequent polymerization with 12-molybdophosphoric acid, the polyelectrolyte multilayer films containing PPy nanoparticles were fabricated. UV–visible absorption spectrocopy, Fourier transform infrared (FTIR) spectroscopy, atomic force microscopy (AFM), transmission electron microscopy (TEM) and cyclic voltammograms (CVs) were used to characterize the PPy nanoparticles and their multilayer thin films. UV–visible spectra indicate that the growth of PPy nanoparticles was regular and occurred within the polyelectrolyte films. The size of prepared PPy nanoparticles was found by TEM to increase with the increasing of polymerization cycles. The electrochemistry behavior of the multilayer thin films was studied in detail on ITO. The results suggest that the LbL adsorption and polymerization method developed herein provides an effective way to prepare PPy nanoparticles in the polymer matrix.

Keywords: Layer-by-layer; Polypyrrole; Ultrathin film

1. Introduction

The construction of nanoparticle-loaded multilayer ultrathin films has generated a great deal of interest for a number of years [1]. Nanometer-sized semiconductor, metal and metal oxide have unusual electronic and optical properties due to the large specific surface area and the quantum size effect, which are not available for the corresponding bulk materials [2,3]. The films containing these nanoparticles hold potential applications for catalysis [4,5], chemical sensors [6,7], optical and electrical devices [8,9] and so on. Among diverse methods to prepare nanoparticles embedded within the polymer matrix, layer-by-layer (LbL) assembly is frequently utilized. The LbL method can allow one to construct a film atop a substrate of almost any kind or shape and to control over film composition and thickness on molecular level [10–17]. This approach providing a simple route to create nanoparticle composite films can be achieved by two ways. One is to adsorb a polyelectrolyte and preformed nanoparticles of an opposite surface charge, but the nanoparticles are liable to aggregation and cannot disperse well in the films. The other is in situ synthesis of nanoparticles, which can be grown selectively and controlled within specific regions of multilayer polyelectrolyte thin film [18–22].

Recently, Stroeve's group has proposed a method of in situ nucleation and growth through LbL assembly to synthesize inorganic nanoparticles in polyelectrolyte multilayer films [23–28]. The polyelectrolyte precursor film provides specific regions for subsequent adsorption and hydrolysis of metallic ions, which is repetitively carried out in aqueous metal salt solutions and aqueous alkali solution. This means has been employed by our group to prepare the multilayer films containing polyoxometalate (POM) nanoparticles and the size and morphology of nanoparticles can be controlled by increasing the adsorption and precipitation cycle numbers [29].

By now, nanoparticles prepared within the ultrathin films have been limited to inorganic species, however, nanosized conductive polymer particles have not been achieved in the polyelectrolyte films although the various doped conjugated polymers multilayer thin films were obtained by LbL assembly [12,30–33]. Among

---

* Corresponding author. Tel.: +86 431 509 8787; fax: +86 431 568 4009.
E-mail address: wangenbo@public.cc.jl.cn (E. Wang).

0032-3861/$ - see front matter © 2005 Elsevier Ltd. All rights reserved.
doi:10.1016/j.polymer.2005.12.002

conducting polymers, polypyrrole (PPy) has many pronounced features related to electrical conductivity, electroactivity and high environmental stability, so it attracts extensive research interests. But it is still a challenge to fabricate PPy films and hence PPy nanoparticle ultrathin films. The reason for that may be PPy always exists in an intractable state and suffers from insolubility in most solvents and poor processability that is not satisfactory for practical application [12,34–41].

In this paper, as a development of the method for in situ nucleation and growth of nanoparticles provided by Stroeve, we achieved conducting polymer—polypyrrole (PPy) nanoparticles with different size in polyelectrolyte multilayer films by the LbL adsorption and polymerization method. 12-Molybdophosphoric anions, in its acidic form—$H_3PMo_{12}O_{40}$ (PMo_{12}), a kind of strong oxidant and acid, is reported to be suitable for oxidizing pyrrole to PPy in the absence of any other reagent. And the achieved PPy has high conductivity with values typically in the range from 1.0 to 0.1 S cm^{-1}. In the case that the reaction was carried out in air, PMo_{12} would act as a catalyst and could be easily reoxidized by molecular oxygen [42–44]. These characteristics of PMo_{12} make it possible for synthesis of PPy nanoparticles within polyelectrolyte films by sequential adsorption from aqueous pyrrole monomer solution and subsequent polymerization with PMo_{12}. The size of the PPy nanoparticles grown in the polymer matrix can be tuned by the number of polymerization cycles.

2. Experimental section

2.1. Chemicals

Poly(diallyldimethylammonium chloride) (PDDA, MW ~ 100,000–2,000,000) and poly(styrenesulfonate) sodium salt (PSS, MW ~ 70,000) were purchased from Aldrich and used as received. Polyoxometalates with the composition $H_3PMo_{12}O_{40}\cdot 14H_2O$ was prepared according to the literature procedure [45]. Pyrrole was distilled and stored under a nitrogen atmosphere before use. All of the other chemicals are of reagent grade.

2.2. Instruments

UV–vis absorption spectra were carried out on a quartz slide using a 756 PC UV–vis spectrophotometer. The FTIR spectra were obtained in the absorbance mode using a Bio-Rad FTS135 spectrophotometer and bare silicon wafer was used as the reference. A Hitachi H-600 microscope was used to collect the TEM micrograph of the PPy–PMo_{12} nanoparticles within films. Surface morphology of the samples was determined on mica by using a Digital Instruments Nanoscope IIIa instrument operating in the tapping mode with silicon nitride tips under ambient conditions. The electrochemical experiments were performed on a CHI 660 electrochemical workstation connected to a digital-586 personal computer by using a conventional three-electrode system. Ag/AgCl was used as the reference electrode, Pt gauze as a counter electrode, and the ITO as working electrode.

2.3. Film formation

The PDDA and PSS solutions were 2 and 1 mg/mL, respectively. The pyrrole monomer was dissolved in aqueous solution with pH = 4 (adjusted with dilute HCl) at a concentration of 0.1 M, in which pyrrole was positively charged. The pristine polyelectrolyte films were prepared by alternately depositing PDDA and PSS on the cleaned quartz slide for 20 min, respectively. Deionized water and HCl solution (pH = 4) were used for rinsing after each immersion step. A PDDA/PSS layer was called a bilayer. And then the polyelectrolyte-modified substrate was dipped into freshly prepared pyrrole monomer solution and PMo_{12} solution (0.01 M) for 1 and 2 min, respectively. Rinsing with deionized water and drying with N_2 were performed after each deposition step. This process was called one polymerization cycle and was repeated after 20 min. The above procedure resulted in the build-up of the multilayer films containing PPy–PMo_{12} nanoparticles, which can be expressed as $(PDDA/PSS)_m$ $(PPy–PMo_{12})_n$, where m is the numbers of polyelectrolyte bilayer and n is the numbers of polymerization cycle.

3. Results and discussion

A possible mechanism of formation for PPy–PMo_{12} nanoparticle by in situ chemical oxidation in the polyelectrolyte films is shown in Scheme 1. Firstly, the polyelectrolyte precursor films were constructed via electrostatic LbL self-assembly. Then, positively charged pyrrole monomers permeated through the pore in the film and were distributed along

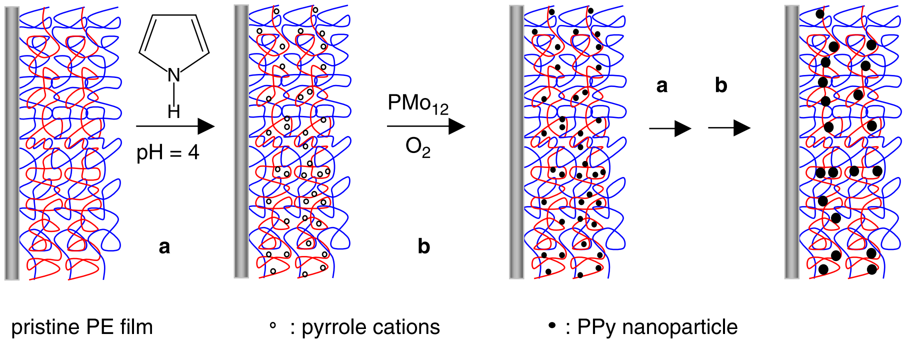

Scheme 1. Schematic representation for the preparation of ultrathin multilayer films containing PPy nanoparticles doped with PMo_{12}.

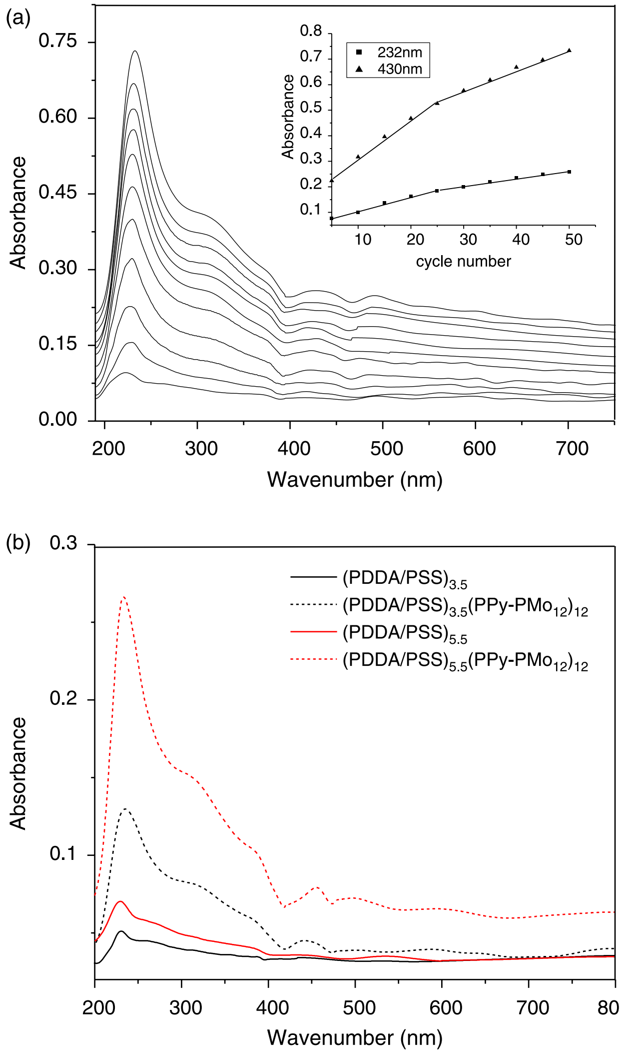

Fig. 1. (a) UV–vis spectra of $(PDDA/PSS)_{5.5}/(PPy–PMo_{12})_n$ films with $n=0\sim50$ on quartz substrates (the interval is five cycles). The inset shows the plots of the absorbance values at 232, 430 nm versus the number of polymerization cycles. (b) UV–vis spectra of multilayer films $(PDDA/PSS)_m$ with $m=3.5$, 5.5 and these two films after 12 adsorption and polymerization cycles.

the PSS chains due to electrostatic attraction. Because the adsorbed pyrrole monomers were limited in the definite region of PDDA/PSS matrix, the formed particles would not aggregate but yielded a small size. On adsorption of PMo_{12} in acidic condition, the polymerization of pyrrole monomers was initiated. Afterward, the pyrrole monomers continue to be deposited on and polymerized following by partial desorption of formed nanoparticle and subsequently the size of which would increase with polymerization cycles [46].

The growth process of multilayer films containing PPy nanoparticles was monitored by UV–vis spectrocopy. Fig. 1 shows the UV–vis spectra of $(PDDA/PSS)_{5.5}$ multilayer films with n polymerization cycles (from 0 to 50). The characteristic bands at 232 and 317 nm are ascribed to the oxygen→molybdenum charge-transfer (CT) transition of $H_3PMo_{12}O_{40}$. The shoulder at about 224 nm is due to the aromatic group of PSS, which indicates that PMo_{12} did not deposit on the PDDA [29]. The broad humps around 430 nm are caused by the electronic transitions from valence band to conduction band of polypyrrole [47]. It should be noted that with the polymerization cycle number n increasing, the absorbance at 430 nm red-shift which is ascribed to the increasing size of $PPy–PMo_{12}$ nanoparticles and the absorption peak at about 490 nm due to the reduction of PMo_{12} anions appeared. The PSS was not chosen as the outmost layer, otherwise the particle growth would be uncontrolled as far as particle size [23]. A plot of the absorbance at 232 and 430 with increasing number of polymerization cycles is shown in Fig. 1(a). It is noteworthy that each curve of different wavelength may be modeled best by two lines of slightly different slope with an inflection point at around the 25th cycle. It indicated that the process including adsorption of pyrrole monomers in the films and subsequent polymerization with PMo_{12} is reproducible in former 25 cycles. After the 25th cycle, although the process is still reproducible, the quantities of pyrrole monomers polymerized decreased. The reason for this decrease may be explained by the partial desorption of previously formed particles during the next adsorption when the size of nanoparticle increased to a certain extent, which is associated with the increase in electrostatic repulsion and the influence of roughness on the particles [46]. In Fig. 1(b), the absorbance of multilayer films containing PPy nanoparticles is shown to increase with the increasing number of polyelectrolyte bilayers. That is to say additional PSS layers enable more pyrrole monomers to bind to the sulfonate groups, which results in an increase in PPy nanoparticles after polymerization. This also shows that the formation of $PPy–PMo_{12}$ nanoparticles occurs in the films and the phenomenon is not a surface effect [23].

Fourier transform infrared (FTIR) spectroscopy was applied for determining the composition of the polyelectrolyte multilayer films containing $PPy–PMo_{12}$ nanoparticles. Fig. 2 shows the FTIR spectrum of the film recorded in the frequency range from 1600 to 600 cm^{-1}. The peaks at 1536 and 1466 cm^{-1} are related to aromatic C=C and C–C, respectively. And the C–N and C=N stretching shows peaks at 1291 and 1189 cm^{-1}

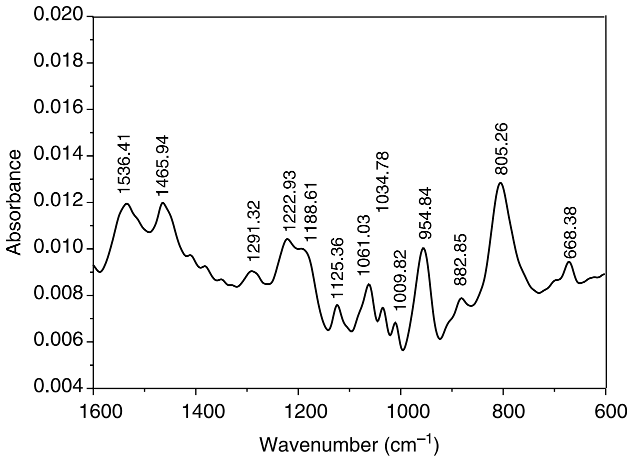

Fig. 2. FTIR spectrum of PDDA/PSS polyelectrolyte multilayer films containing $PPy–PMo_{12}$ nanoparticles assembled on the silicon wafer.

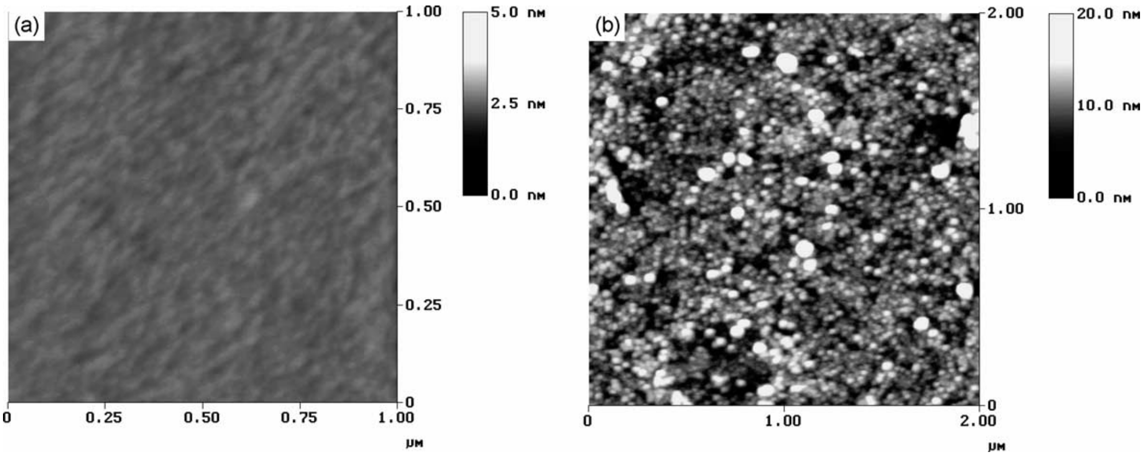

Fig. 3. Tapping mode AFM image of $(PDDA/PSS)_{3.5}$ before (a) and after (b) three polymerization cycles assembled on mica.

[48,49]. The above absorption data indicate the formation of PPy. The characteristic bands at 1061.03, 954.84, 882.85, and 805.26 cm^{-1} should be ascribed to the vibration modes of ν(P=Oa[1]), ν(Mo=Ot), ν(Mo–Ob–Mo) and (Mo–Oc–Mo), respectively. In addition, the feature peaks at 1222.93, 1125.36, 1034.78, 1009.82 cm^{-1} showed the presence of PSS. Thus, all these FTIR data provide supportive evidence that pyrrole monomers have been polymerized to PPy with PMo_{12} in the PDDA/PSS system, which is consistent with data of the UV–vis spectra.

The information concerning the surface morphology of the PPy nanoparticle thin films was obtained by atomic force microscopy (AFM) in tapping mode. Fig. 3 shows the surface topology of (PDDA/PSS) 3.5 multilayer films before (a) and after (b) three polymerization cycles assembled on mica. It is obvious that the surface of thin films containing PPy nanoparticles is rougher than that of the PDDA/PSS pristine films. From Fig. 3(b), it is clearly seen that the circular particles with nearly equal size are well dispersed on the polyelectrolyte surface and these circular particles are attributed to the formation of PPy nanoparticles in the polyelectrolyte multilayer films. It can be deduced from the AFM image that the thin polymer films containing well-defined PPy nanoparticles could be achieved by this LbL adsorption and polymerization means.

To further understand the detailed structure of the multilayer films containing PPy nanoparticles, the transmission electron microscopy (TEM) spectroscopy was carried out. Fig. 4 provides the TEM micrographs of the variation of a 3.5 bilayer PDDA/PSS film in the process of PPy nanoparticle formation. From the figures, it can be seen that the size of the PPy nanoparticles is determined by the number of polymerization cycles. For the polymerization cycle number $n=3$, PPy has spherical shape with a diameter ranging from 20 to 40 nm (Fig. 4(a)). The PPy structure is much better resolved after further polymerization. Fig. 4(b) is the TEM micrograph of $n=6$, the final PPy nanoparticles exhibit darker inner and several of them grew into strings. The size of PPy is from 75 to 135 nm in diameter. These results suggest that the size of PPy nanoparticles augmented with the increasing of polymerization cycle number not only in horizontal but in normal growth mode. The initially formed PPy nanoparticles can be regarded as the core for the following growth of the PPy.

The electrochemistry of PPy–PMo_{12} nanoparticles ultrathin films was investigated by fabricating the films on ITO. Fig. 5(a) shows the cyclic voltammograms of $(PDDA/PSS)_{3.5}$ multilayer films after 6 polymerization cycles in an aqueous solution of pH=0 H_2SO_4 at scan rate=10 mV/s. There are three pairs of redox peaks between −100 and 600 mV and the formal potentials $E_{1/2}=(E_{pa}+E_{pc})/2$ for the three pairs of peaks are 364 mV (I-I′), 210 mV (II-II′), −27 mV (III-III′), respectively. Redox peaks I-I′, II-II′ and III-III′ correspond to three consecutive two-electron processes. Although the shape of the peaks is similar to that of $(PDDA/PSS)_{3.5}/(TBAB_3/PMo_{12})_6$ multilayer films on ITO electrode in an aqueous solution of 0.5 M H_2SO_4 (see supplement materials S1, TBAB=tetrabutylammonium bromide) [29], it is obvious that the substrate current response is larger at the PPy nanoparticles modified film electrode. This was surely due to the conductive polymer existing in the former multilayer films. Fig. 5(b) is the CVs of polyelectrolyte pristine films with different bilayer numbers after 6 polymerization cycles. It can be seen from the figure that the peak current of $(PDDA/PSS)_m/(PPy–PMo_{12})_6$ with $m=3.5$ is well-defined and higher than the other two. It has been proved that the polymerization process occurred within the films and the increase of polyelectrolyte layers can result in more PPy–PMo_{12} nanoparticles formed. So, the peak current with $m=3.5$ is stronger than that with $m=1.5$. But, the peak current decreased obviously when $m=6.5$ that more polyelectrolyte layers has been deposited. This may be due to so much polyelectrolyte was adsorbed and the strong electrostatic interaction may repel diffusion of protons to the PMo_{12} entrapped in PPy and then the current decreased.

---

[1] Oa, oxygen in P–O tetrahedron; Ot, terminal oxygens; Ob, bridging OM2 oxygens; Oc, central OM6.

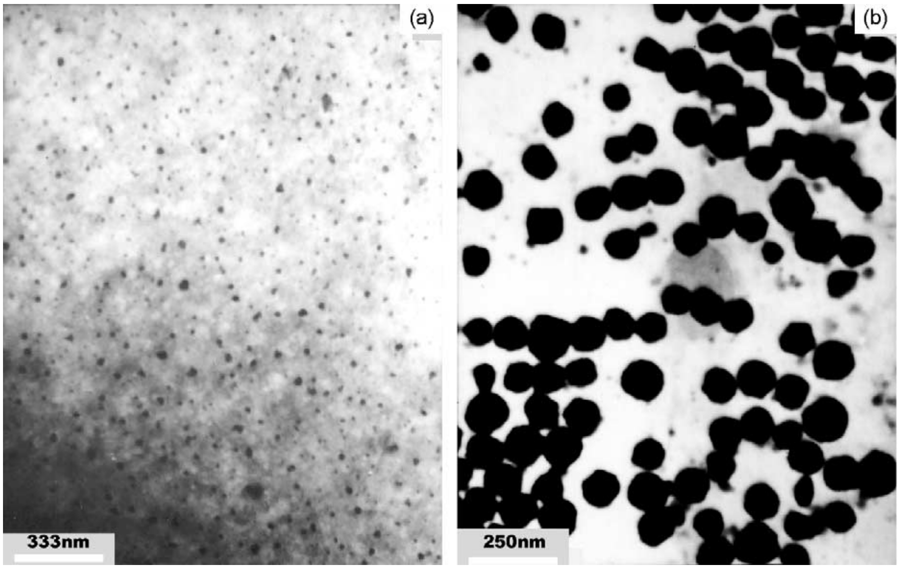

Fig. 4. TEM micrographs of 3.5-bilayer films of PDDA and PSS after different *n* polymerization cycles (a) $n=3$; (b) $n=6$.

Fig. 5(c) represents the dependence of formal potentials $E_{1/2}$ of the multilayer films $(PDDA/PSS)_{3.5}/(PPy–PMo_{12})_3$ on different solution pH. It can be seen that the three pairs of redox peaks shift negatively with increasing pH, as expected according to the Nernst equation. $E_{1/2}$/pH slope values in the three curves are −48, −67 and −62 mV/pH, respectively, which are close to the theoretical value of −59 mV/pH for a $2e^-/2H$ redox process [47,50].

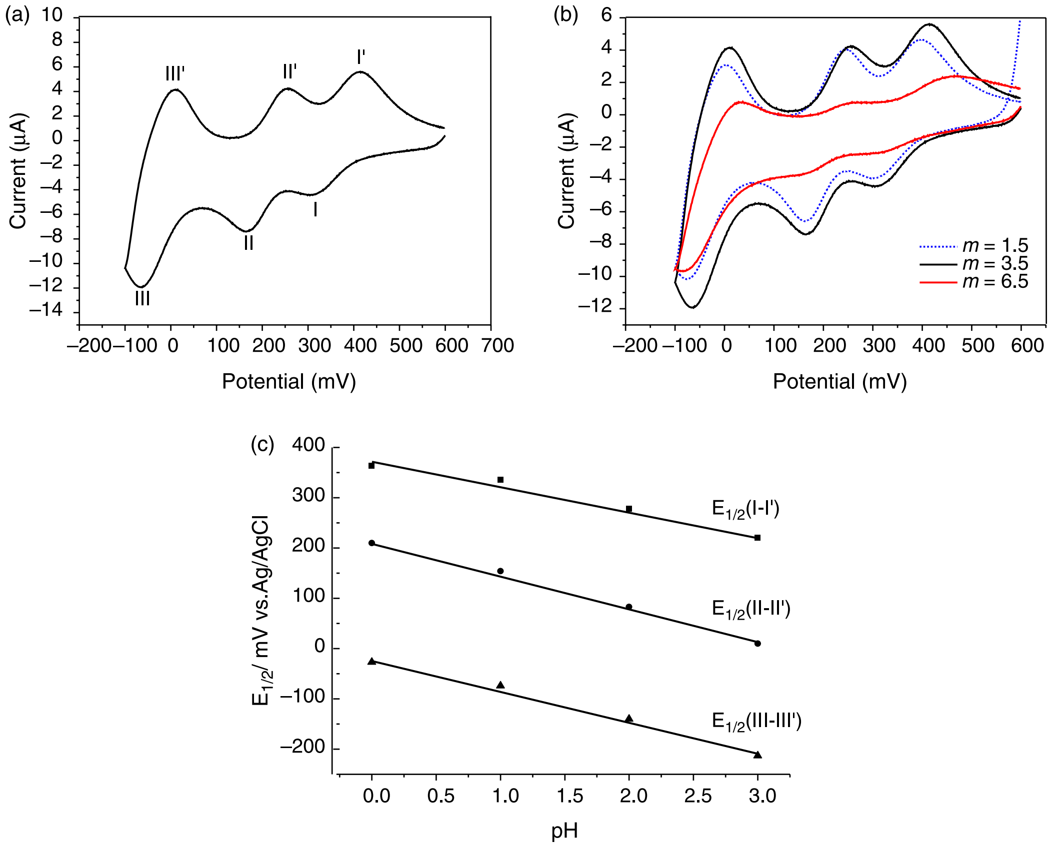

Fig. 5. (a) Cyclic voltammograms of $(PDDA/PSS)_{3.5}/(PPy–PMo_{12})_6$ films on ITO electrode in an aqueous solution of $pH=0$ H_2SO_4 (I: the first reductive peak; I′: the first oxidative peak); (b) cyclic voltammograms of polyelectrolyte pristine films $(PDDA/PSS)_m$ with different *m* layers after 6 polymerization cycles in an aqueous solution of $pH=0$ H_2SO_4; (c) relationships between peak potential and pH, buffer solution is 0.2 M $Na_2SO_4+H_2SO_4$. Scan rate: 10 mV/s Potentials vs. Ag/AgCl.

4. Conclusions

In conclusion, we demonstrated a kind of LbL adsorption and polymerization method by extending the in situ nucleation and growth of nanoparticles in polyelectrolyte provided by Stroeve. This method enables solution-based preparation of PPy nanoparticles in ultrathin films. The polymerization of PPy occurs within the polyelectrolyte multilayer films and the size of PPy nanoparticles can be controlled by the number of polymerization cycles. The related CV studies indicate that the films have good voltammetric response in $\mathrm{pH} \leq 3$ buffer and the pH of supporting electrolyte and the numbers of polyelectrolyte layers have influence on their electrochemistry behavior. This approach provides an effective route to construct PPy nanoparticle multilayer films. And owing to the characteristics of PMo_{12} acid—strongly oxidizing species and strong acid, the preparation of other kinds of conducting polymer nanoparticles ultrathin films by this method is expected to be possible.

Acknowledgements

This work was financially supported by the National Natural Science Foundation of China (20371011).

Supplementary data

Supplementary data associated with this article can be found at doi:10.1016/j.polymer.2005.12.002

References

[1] Fendler JH. Nanoparticles and nanostructured films: preparation, characterization and applications. Weinheim: Wiley–VCH; 1998.
[2] Fendler JH, Meldrum FC. Adv Mater 1995;7(7):607–32.
[3] Weller H. Angew Chem Int Ed Engl 1993;32(1):41–53.
[4] Kidambi S, Dai JH, Li J, Bruening ML. J Am Chem Soc 2004;126(9):2658–9.
[5] Espinal L, Suib SL, Rusling JF. J Am Chem Soc 2004;126(24):7676–82.
[6] Matsui J, Akamatsu K, Hara N, Miyoshi D, Nawafune H, Tamaki K, et al. Anal Chem 2005;77(13):4282–5.
[7] Yu A, Liang Z, Cho J, Caruso F. Nano Lett 2003;3(9):1203–7.
[8] Kietzke T, Neher D, Kumke M, Montenegro R, Landfester K, Scherf U. Macromolecules 2004;37(13):4882–90.
[9] Tseng RJ, Huang J, Ouyang J, Kaner RB, Yang Y. Nano Lett 2005;5(6):1077–80.
[10] Cho JH, Lee SH, Kang H, Char K, Koo J, Seung BH, et al. Polymer 2003;44(18):5455–59.
[11] Decher G. Science 1997;277(5330):1232–7.
[12] Fou AC, Rubner MF. Macromolecules 1995;28(21):7115–20.
[13] Zhang X, Shen JC. Adv Mater 1999;11(13):1139–43.
[14] Liu SQ, Kurth DG, Bredenkötter B, Volkmer D. J Am Chem Soc 2002;124(41):12279–87.
[15] Moriguchi I, Fendler JH. Chem Mater 1998;10(8):2205–11.
[16] Liu SQ, Kurth DG, Möhwald H, Volkmer D. Adv Mater 2002;14(3):225–8.
[17] Lan Y, Wang EB, Song YH, Kang ZH, Jiang M, Gao L, et al. J Colloid Interface Sci 2005;284(1):216–21.
[18] Dai JH, Bruening ML. Nano Lett 2002;2(5):497–501.
[19] Wang TC, Rubner MF, Cohen RE. Chem Mater 2003;15(1):299–304.
[20] Wang TC, Rubner MF, Cohen RE. Langmuir 2002;18(8):3370–5.
[21] Joly S, Kane R, Radzilowski L, Wang T, Wu A, Cohen RE, et al. Langmuir 2000;16(3):1354–9.
[22] Lee D, Rubner MF, Cohen RE. Chem Mater 2005;17(5):1099–105.
[23] Dante S, Hou ZZ, Risbud S, Stroeve P. Langmuir 1999;15(6):2176–82.
[24] Zhang LQ, Dutta AK, Jarero G, Stroeve P. Langmuir 2000;16(17):7095–100.
[25] Dutta AK, Jarero G, Zhang LQ, Stroeve P. Chem Mater 2000;12(1):176–81.
[26] Dutta AK, Ho T, Zhang LQ, Stroeve P. Chem Mater 2000;12(4):1042–8.
[27] Fojas AM, Murphy E, Stroeve P. Ind Eng Chem Res 2002;41(11):2662–7.
[28] Stroeve P. Nucleation of nanoparticles. Ultrathin polymer films in encyclopedia of nanoscience nanotechnology. New York: Marcell Dekker; 2004 p. 2713–19.
[29] Lan Y, Wang EB, Song YH, Kang ZH, Xin L, Li Z, et al. New J Chem 2005;29(10):1249–53.
[30] Ferreira M, Rubner MF. Macromolecules 1995;28(21):7107–14.
[31] Cheung JH, Stockton WB, Rubner MF. Macromolecules 1997;30(9):2712–6.
[32] Stockton WB, Rubner MF. Macromolecules 1997;30(9):2717–25.
[33] Wakizaka D, Fushimi T, Ohkita H, Ito S. Polymer 2004;45(25):8561–5.
[34] Zheng SP, Tao C, He Q, Zhu HF, Li JB. Chem Mater 2004;16(19):3677–81.
[35] Neoh KG, Teo HW, Kang ET. Langmuir 1998;14(10):2820–6.
[36] Park MK, Onishi K, Locklin J, Caruso F, Advincula RC. Langmuir 2003;19(20):8550–4.
[37] Ram MK, Adami M, Paddeu S, Nicolini C. Nanotechnology 2000;11(2):112–9.
[38] Jang J, Oh JH. Langmuir 2004;20(20):8419–22.
[39] Ram MK, Adami M, Faraci P, Nicolini C. Polymer 2000;41(20):7499–509.
[40] Pich A, Lu Y, Boyko V, Arndt KF, Adler HJP. Polymer 2003;44(25):7651–9.
[41] Bae WJ, Kim KH, Jo WH, Park YH. Polymer 2005;46(23):10085–91.
[42] Gómez-Romero P, Lira-Cantú M. Adv Mater 1997;9(2):144–7.
[43] Lira-Cantú M, Gómez-Romero P. Chem Mater 1998;10(3):698–704.
[44] Gómez-Romero P. Adv Mater 2003;13(3):163–74.
[45] Filowitz M, Ho RKC, Klemperer WG, Shum W. Inorg Chem 1979;18(1):93–103 [References therein].
[46] Kotov NA. In: Decher G, Schlenoff JB, editors. Multilayer thin films-sequential assembly of nanocomposite materials. Weinheim: Wiley–VCH; 2003. p. 216–7.
[47] Dong SJ, Jin W. J Electroanal Chem 1993;354(1–2):87–97.
[48] Ham HT, Choi YS, Jeong N, Chung IJ. Polymer 2005;46(17):6308–15.
[49] Kim JW, Liu F, Choi HJ, Hong SH, Joo J. Polymer 2003;44(1):289–93.
[50] Zou XQ, Shen Y, Peng ZQ, Zhang L, Bi LH, Wang YL, et al. J Electroanal Chem 2004;566(1):63–71.